Viscoelastic properties of polystyrene/polyamide-6 blend compatibilized with silica/polystyrene Janus hybrid nanoparticles

A. S. Caro-Bretelle, T. Parpaite, B. Otazaghine, A. Taguet, J. M. Lopez-Cuesta

▶ **To cite this version:**

A. S. Caro-Bretelle, T. Parpaite, B. Otazaghine, A. Taguet, J. M. Lopez-Cuesta. Viscoelastic properties of polystyrene/polyamide-6 blend compatibilized with silica/polystyrene Janus hybrid nanoparticles. Journal of Rheology, 2017, 61 (2), pp.305-310. 10.1122/1.4975334 . hal-02892738

HAL Id: hal-02892738
https://hal.science/hal-02892738

Submitted on 15 Dec 2020

HAL is a multi-disciplinary open access archive for the deposit and dissemination of scientific research documents, whether they are published or not. The documents may come from teaching and research institutions in France or abroad, or from public or private research centers.

L'archive ouverte pluridisciplinaire **HAL**, est destinée au dépôt et à la diffusion de documents scientifiques de niveau recherche, publiés ou non, émanant des établissements d'enseignement et de recherche français ou étrangers, des laboratoires publics ou privés.

Viscoelastic properties of polystyrene/polyamide-6 blend compatibilized with silica/polystyrene Janus hybrid nanoparticles

A. S. Caro,[a] T. Parpaite, B. Otazaghine, A. Taguet, and J. M. Lopez-Cuesta

Centre des Matériaux des mines d'Alès, 6, avenue de Clavières, 30319 Alès, France

Abstract

The greatest challenge in the field of multiphase polymer blend research is the compatibility of the phases, which is responsible for the overall microstructure. The control of the interfacial interactions between the components is therefore a necessity. Here, we investigate the compatibilization in a polystyrene/polyamide-6 (PS/PA6) blend. Silica/polystyrene Janus hybrid nanoparticles (JHNPs) were synthesized and used as compatibilizing agents in PS/PA6 blends. Four levels of incorporation were tested (1.5, 3, 5, and 10 phr) in a PS/PA6 (80/20 wt. %) blend. Due to their intrinsic amphiphilic properties, the JHNPs migrate to the interface of the PS/PA6 blend. We demonstrate that silica/polystyrene JHNPs act as compatibilizing agents in PS/PA6 blends. These nanoparticles allow the combination of a "Pickering effect" of a solid particle with a "copolymer effect." Microscopic analysis confirms the emulsifying ability of these asymmetric nanoparticles. Rheological measurements show an increase in the viscosity with the level of particle incorporation. Relaxation spectra reveal additional peaks (related to slower process) as JHNPs are added into the pristine blend. These peak occurrences can be related, via modeling, to interfacial tension. The compatibilizing effect of the JHNPs is confirmed by a decrease in interfacial tension up to 5 phr of particles.

I. INTRODUCTION

Polymer blend is a relevant way to generate materials with outstanding properties in comparison with the neat polymers. Most of the polymer blends show immiscible systems with properties depending crucially on their composition, on the blend morphology, and on their components interactions. Hence, the control of both blend morphology and interfacial adhesion between the polymeric components through compatibilization is challenging. In a previous study, Janus hybrid nanoparticles (JHNPs) were used to compatibilize polystyrene/polyamide (PS/PA6) blends [1]. JHNPs were synthesized at the gram scale via miniemulsion polymerization technique. In PS/PA6 80/20 blends, JHNPs were clearly located at the polymer interface allowing compatibilization to be improved and entailing an emulsification effect. The compatibilization ability was quantified via interfacial tension data. They were obtained through indirect measurements using rheological data at the molten state from simplified Palierne theory (neglecting interfacial viscoelasticity). Nevertheless the modeling carried out had a very sensitive response in the low-frequency zone, and the dispersed phase volume fraction has been adapted to take into account the viscosity increase in the full-frequency range due to the presence of JHNPs at the interface.

In this work, the compatibilization capability is studied from the relaxation spectrum which is numerically computed from rheological measurements. Some authors [2] used specific relaxation times [matrix, droplets, interphase (associated with a longer time)] and the Palierne's theory to deduce the interfacial tension. A frequency-independent interfacial moduli as well as a monomodal dispersed domain size distribution is assumed. Many authors were able to qualify the miscibility degree of various polymers via this model (PP/HDPE [3], PPT/m-LLDPE [4], PP/PA6 [5,6], PET/PA66 [7], PLA/PETG [8], PP/EVA [9], and EVA/PETG [10]). In the case of complex morphology [existence of emulsion in emulsion (EE) structure], the Palierne's model failed [5].

In the present study, PS/PA6 blends at ratio 80/20 were prepared by melt compounding. JHNPs were used as potential compatibilizer for the blends. The influence of JHNPs (1.5, 3, 5, and 10 phr) on morphology and blends rheological response was investigated. An adaptation of the Palierne theory was used to deduce the interfacial tension from the relaxation spectra.

II. MATERIALS AND METHODS

A. Materials

CRISTAL 1340 polystyrene (PS) was supplied by Total Petrochemicals (Feluy, Belgium). It has a high molecular weight, a melt flow index (MFI) of 4 g·10 min^{-1} (with 5 kg at 200 °C), and a density of 1.05 g/cm^3. Aquamid AQL40 polyamide-6 (PA6) was supplied by Aquafil Technopolymers (Arco, Italy). Its melting point is 220 °C (ISO Test Method 3146), its MFI is 160 g·10 min^{-1} (with 5 kg at 275 °C), and its density is 1.14 g/cm^3. Polymer pellets were dried under vacuum at 80 °C for 12 h before processing.

[a]Author to whom correspondence should be addressed; electronic mail: Anne-Sophie.Caro@mines-ales.fr

The JHNPs used in this work consist of a silica nanoparticle around 50 nm diameter with only one hemisphere graft by PS chains resulting in a PS nodule around 80 nm diameter. Our protocol is a two-step procedure based on the pioneering work of Lu *et al*. [11] who were the first to report the one-pot synthesis of such kind of hybrid asymmetric nanoparticles. The full synthesis procedure is well described in a previous work [1]. As an example, the image of a JHNP is presented in Fig. 1. To avoid handling of dry nanoparticles powders, we used in a first step a solvent casting method to embed Janus nanoparticles into the PS film. PS pellets of 1 g was dissolved in 10 ml of Tetrahydrofuran (THF) and mixed with desired quantities of JHNPs at room temperature during 12 h under magnetic stirring. The solvent was then evaporated at room temperature, and the obtained film was dried under vacuum at 80 °C for 3 h.

B. Preparation of blends

Melt compounding was carried out using a *mini* twin-screw extruder with three steps. During 1 min, PS pellets were first introduced followed by the PS film containing JHNPs and finally PA6 pellets (the screw speed is maintained at 60 rpm). The mixing was carried out for 4 min at 250 °C with a constant screw speed (120 rpm). Finally, the wire was extruded at a screw speed of 40 rpm. All formulations were performed under nitrogen. Blends having PS/PA6 composition of 80/20 were prepared. Ternary blends PS/PA6/JHNPs were prepared by adding 1.5, 3, 5, and 10 wt. % of JHNPs. The blend pellets and JHNPs were dried under vacuum at 80 °C for 12 h before processing. For rheological measurements, the pellet samples with a thickness of 1.5 mm and a diameter of 25 mm were obtained by an IM15 Zamak Mercator laboratory injection machine. The injection temperature and injection pressure were 250 °C and 3.5 bars, respectively.

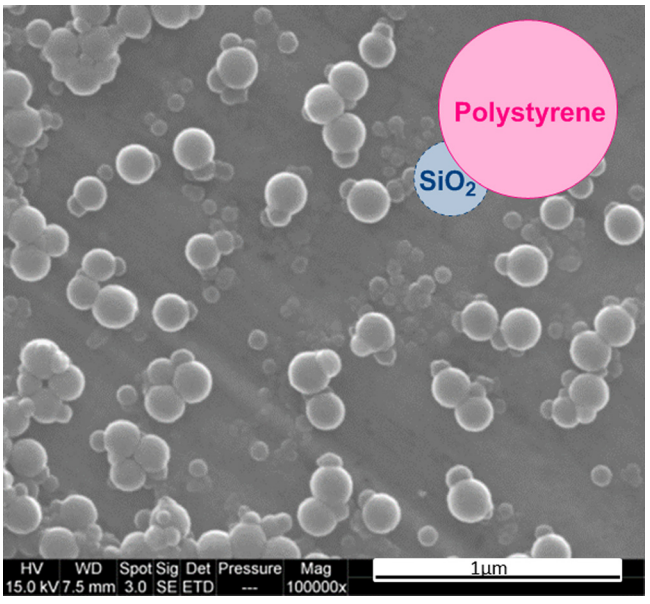

FIG. 1. SEM image of a hybrid Janus nanoparticle synthesized by a miniemulsion process [1].

C. Characterizations

1. Dynamic rheology

The rheological properties of the blends were evaluated by oscillatory characterization on a Rheometric Scientific ARES rheometer (TA instrument) equipped with parallel plate geometry (plate diameter 25 mm and gap 1 mm). All experiments were carried out at 230 °C under nitrogen to avoid polymer degradation and absorption of moisture. The storage G′, the loss moduli G″, and the viscosity η of the samples were measured with constant strain oscillatory tests within the linearity limit for all blends: A frequency range ω from 100 to 0.01 rad/s and a strain of 3% were applied during the measurements. A strain sweep was applied to fix the strain limit for the linear viscoelastic response.

2. Scanning electron microscopy

Morphologies of the PS/PA6/Janus blends were observed with a scanning electron microscope (SEM) (FEI Quanta 200 ESEM) under an accelerating voltage of 15 kV. Samples were fractured in liquid nitrogen, and the cross-section was observed. Then, the state of dispersion and distribution of PA6 nodules in the PS matrix and the impact of Janus nanoparticles incorporation were studied. A thin layer of carbon around 15 nm was deposited on all samples before observation to enhance conductivity.

3. Laser diffraction particle size analyzer

A Coulter LS 13230 (Coulter Beckmann, Co.) laser diffraction particle size analyzer was used to determine the particle size diameter of extracted PA6 nodules. The PA6 nodules were collected after dissolving the PS matrix using THF solvent. Particle size measurements were performed using the microliquid module (MLM, 15 ml) in THF, and obscuration was $10 \pm 2\%$. At least, three measurements were performed for each sample. This protocol was fully detailed in a previous paper [12].

4. Modeling

Continuous relaxation spectra offer an efficient way to qualify the material viscoelasticity revealing aspects of its behavior that may not be obvious in plots of the storage and loss moduli. It reflects the molecular movements of macromolecules (giving the weight of molecular relaxation time) and can be related to molecular structure and properties. Nevertheless, it is not possible to measure directly a relaxation spectrum. It can be only calculated on the basis of experimental data. Storage and loss modulus can be expressed as a function of relaxation spectrum H through following equations:

$$G'(\omega) = \int_{-\infty}^{+\infty} H(\tau) \frac{\omega^2\tau^2}{1+\omega^2\tau^2} d\ln\tau, \tag{1}$$

$$G''(\omega) = \int_{-\infty}^{+\infty} H(\tau) \frac{\omega\tau}{1+\omega^2\tau^2} d\ln\tau, \tag{2}$$

where τ is the relaxation time. The evaluation of H from Eqs. (1) and (2) is not straightforward since it is a solution of

a very ill-defined problem. Many publications have studied the best way to obtain it. We used a nonlinear Tikhonov regularization via a MATLAB implementation—the algorithm is fully described in [13]. Times associate with maximum weight in relaxation spectrum plot can be related to microstructure: For blends exhibiting a two phase microstructure, specific relaxed times can be linked to the relaxation of the droplet phase and even to the relaxation of the interphase matrix/droplets. As soon as the interface is assumed to have its own behavior (described by its surface shear and dilatation moduli), Palierne's theory enables the prediction of blend viscoelasticity [14]

$$G_b^*(w) = G_m^*(w)\left[\frac{1+3\int_0^\infty \frac{E(w,R)}{D(w,R)}\nu(R)dR}{1-2\int_0^\infty \frac{E(w,R)}{D(w,R)}\nu(R)dR}\right], \qquad (3)$$

where

$$E(w,R) = \left[G_d^*(w) - G_m^*(w)\right]\left[19G_d^*(w) + 16G_m^*(w)\right] + \frac{4\alpha}{R}\left[5G_d^*(w) + 2G_m^*(w)\right] + \frac{\beta''(w)}{R}\left[23G_d^*(w) - 16G_m^*(w)\right] + \frac{2\beta'(w)}{R}\left[13G_d^*(w) + 8G_m^*(w)\right] + \frac{24\beta''(w)\alpha}{R^2} + 16\beta'(w)\frac{\alpha+\beta''(w)}{R^2}, \qquad (4)$$

where $G_b^*(w)$ is the complex modulus of the blend, $G_d^*(w)$ is the complex modulus of the dispersed phase, $G_m^*(w)$ is the complex modulus of the matrix, $\beta'(w)$ is the surface shear modulus, $\beta''(w)$ is the surface dilatation modulus, R is the dispersed particle radius. $\nu(R)$ is the distribution function of dispersed particles radius, α is the interfacial tension, and w is the angular frequency.

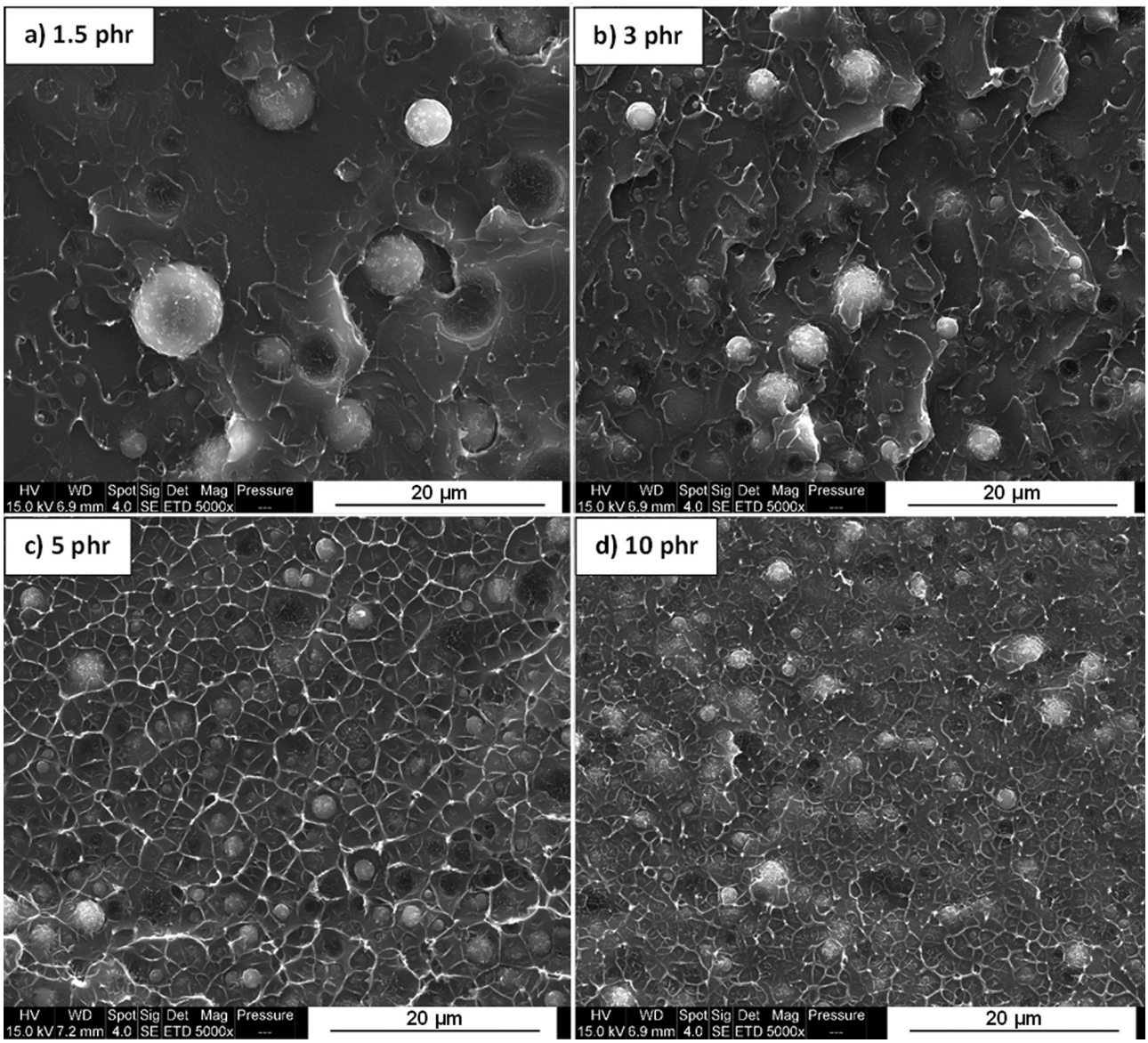

FIG. 2. SEM micrographs of PS/PA/JHNPs 80/20/X systems (X = 1.5, 3, 5, and 10 phr) revealing particles agglomeration since 5 phr of JHNPs (the scale bar is 20 μm).

Jacobs *et al*. [2] simplified this previous version with a frequency independent interfacial moduli and monomodal particle size distribution. Provided the characteristic times of droplet λ_d and interphase λ_{int} can be extracted from relaxation spectrum, the surface dilatation modulus, the shear moduli, and the interfacial tension could be known through Jacobs's developments.

Assuming that λ_d and λ_{int} are independent of β'' and α, respectively [15], and that $\beta' = 0$ (the nodules remain spherical during the process) [16], their expressions can be simplified as

$$\lambda_d = \frac{D_v \eta_m}{8\alpha} \frac{(19p+16)(2p+3-2\phi(p-1))}{10(p+1)-2\phi(5p+2)}, \quad (5)$$

$$\lambda_{int} = \frac{D_v \eta_m}{8\beta''} \frac{10(p+1)-2\phi(5p+2)}{1-\phi}, \quad (6)$$

where η_m is the matrix viscosity, p is the ratio of the droplet viscosity to the matrix viscosity, and ϕ is the dispersed volume fraction. One can deduce the interfacial tension α as soon as λ_d and λ_{int} are known.

III. RESULTS AND DISCUSSION

A. Microstructural characterization

Structural morphological blends evolutions were observed by SEM micrographs on cryofractured samples after dynamical tests (Fig. 2). The diminution of nodules diameters is clearly observed when the content of Janus nanoparticles is increased. Moreover, as expected, asymmetric JHNPs are located at the interface of the PS/PA6 polymer blend due to their amphiphilic character.

After processing, the size distribution of PA6 dispersed phase in the different 80/20 blends was determined by laser diffraction. The PA6 nodules were collected at the end of the rheological test after dissolving the PS matrix using THF. The results in Table I confirm that the incorporation of Janus nanoparticles decreases the median diameter of the PA6 nodules (at least up to 5 phr), leading to an emulsification effect. From 5 phr, the observed increase in the median diameter could be explained by the saturation of the interface by the JHNPs [17] and/or by the creation of a solid network.

B. Rheological properties

The linear viscoelastic properties of molten PS/PA6 blends were measured as a function of frequencies from 100 to 0.01 rad/s; measurements at very low frequencies are of a great interest for the modeling since the interfacial effects are expected to be predominant. Nevertheless, these measurements are associated with very long experiments, thus questioning the *in situ* polymer degradation during experiment. The dynamic viscoelasticity properties were determined at 1 Hz at a prescribed strain (3%) during 25 min. The results presented in Fig. 3 assess the polymer stability at least during the first 25 min. To check that the polymers undergo linear viscoelasticity, a strain scan has been performed until 100% of strain. Figure 4 confirms the linear behavior up to 10% of strain.

Figure 5 presents the evolution of dynamic storage modulus versus frequencies for the neat polymers, the 80/20 PS/PA6 blend, and the blends with various contents of Janus particles (1.5, 3, 5, and 10 phr) at 230 °C and 3% strain. At high frequencies, the blend viscoelastic responses are framed by the ones of neat polymers. It is not the case for lower frequencies: The sample with 10 phr of JHNPs exhibits even a solidlike behavior (plateau at low frequencies for the storage modulus). This phenomenon is in accordance with the morphological characterizations presented above. We assume that this well-known behavior at low frequency arises from the presence of a network structure formed by JHNPs and partly entangled polymer chains adsorbed on the nanoparticles surface [18].

TABLE I. Size distributions of PA6 nodules: Average diameters D_v measured by laser diffraction.

PS/PA/Janus 80/20/x	x = 0 phr	x = 1.5 phr	x = 3 phr	x = 5 phr	x = 10 phr
$D_v(\mu m)$	13.3	12.7	7.8	7.2	9.0

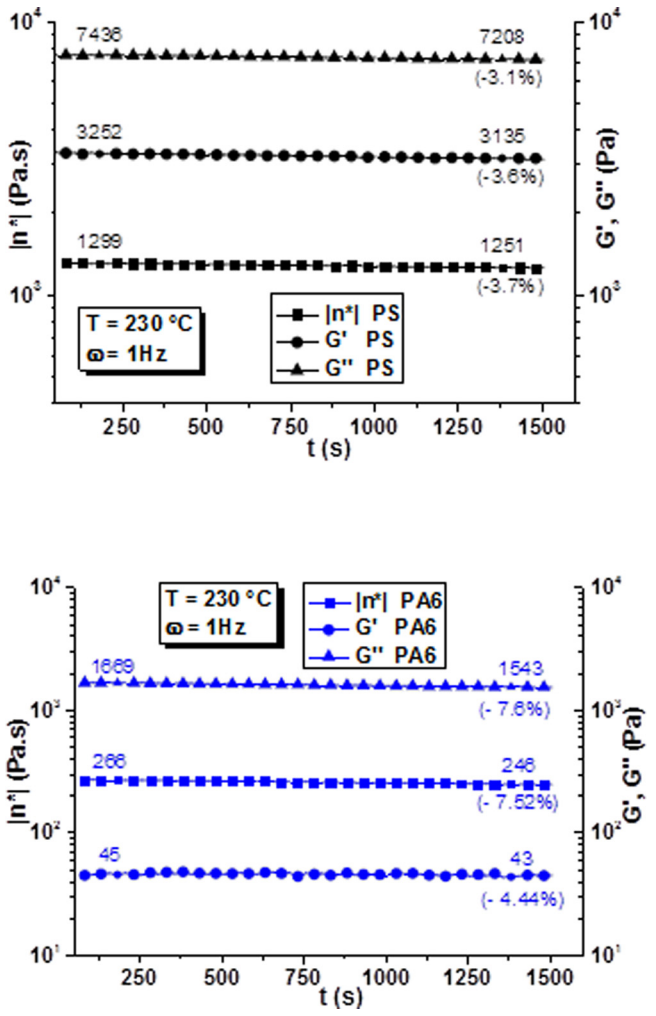

FIG. 3. Rheological stability: Variation of the dynamic storage, loss moduli, and the complex viscosity versus time for the neat PS (left) and PA6 (right) at 230 °C.

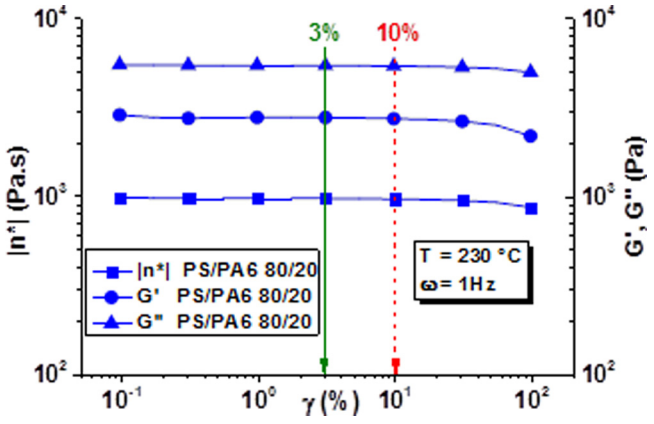

FIG. 4. Linear viscoelasticity: Variation of the dynamic storage, loss moduli, and the complex viscosity versus strain for the 80/20 PS/PA blend at 230 °C.

The weighted relaxation spectra $\lambda H(\lambda)$ versus relaxation time λ of the PS/PA6 blends at 230 °C (Fig. 6) was obtained from Eqs. (1) and (2). As expected, pristine PS and PA6 depict single peaks at 0.19 and 0.32 s, which are their characteristic relaxation times. For the neat blend, two relaxation peaks are clearly observed at about 0.19 and 6.6 s. The first peak corresponds to the relaxation of PS matrix; the second one (which is a slower process) could correspond to the shape relaxation of the dispersed PA6 phase. This relaxation time is noted, λ_d (Fig. 6).

As soon as JHNPs are incorporated in the PS/PA6 blend, another relaxation time appears, λ_{int}, much longer than the precedent (after 100 s): It corresponds to the interphase relaxation. The height of the spectrum is clearly dependent on particles concentration. For the formulation PS/PA6/Janus 80/20/1.5, this additional peak is not detected. According to the corresponding SEM micrograph [see Fig. 2(a)], it is possible that the Janus particles are not incorporated in enough quantity to conduct to an interphase relaxation [19]. From 1.5 phr of JHNPs, λ_d decreases when increasing Janus fraction (Table II). This decrease is

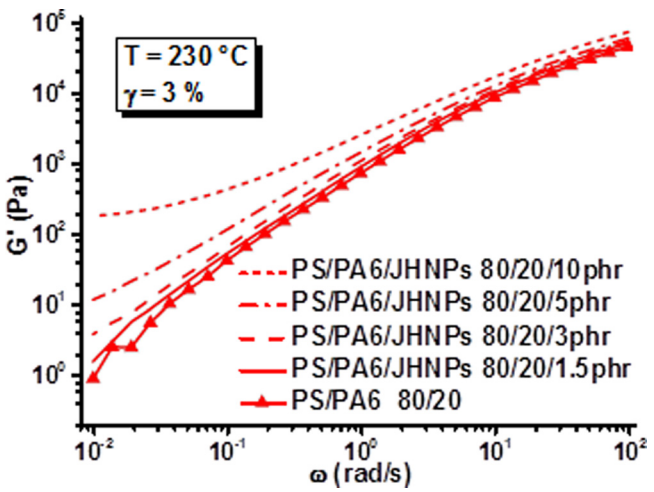

FIG. 5. Storage modulus G′ vs frequencies for the 80/20 PS/PA blend and the ternary blends with various contents (1.5, 3, 5, and 10 phr) of JHNPs, at 230 °C. Determination of interfacial tension from rheological measurements.

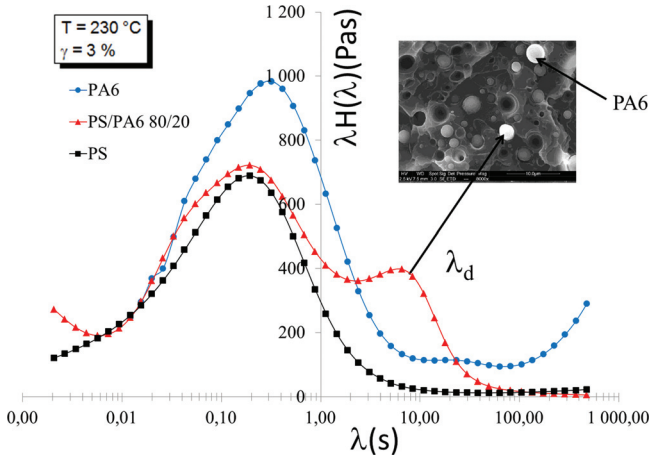

FIG. 6. Weighted relaxation spectra of neat PS, neat PA6 and PS/PA6 80/20 blend at 230 °C.

expected since the nodules diameters decrease with increasing JHNPs content [20] (Fig. 7).

The values of interfacial tension and interfacial shear modulus are summarized in Table II. For the native blend, the interfacial tension value was found to be 7.84 mN/m, which is consistent with the results of both Xing *et al.* [21] (7.1 mN/m for a similar PS/PA6 80/20 system at 230 °C) and team's previous research (6.4 mN/m). After that, the interfacial tension decreases with increasing Janus concentration up to 5 phr. For 10 phr of JHNPs, this parameter increases. This could be associated with agglomeration phenomena and/or a solid network formation. Many authors indicated that in the case of agglomerate systems (which is the case with 10 phr Janus), emulsion models such as the Palierne one cannot be successfully applied [22–24]. The interfacial tension diminution is less pronounced for the 3 and 5 phr JHNPs formulations (in comparison with the 1.5 phr one) because of the formation of the network, already visible on the micrographs.

IV. CONCLUSION

The JHNPs demonstrated effective compatibilization ability in PS/PA6 blend owing to their amphiphilic character. Extrusion/injection processes yielded a multiscale blend morphology with a "raspberry-like" structure of Janus nanoparticles covering PA6 phases in the PS matrix. The efficiency of JHNPs compatibilization was evaluated directly by droplets size evaluation and indirectly by modeling the interfacial tension. The results show a significant reduction of the

TABLE II. Interfacial tension and relaxation modulus for PS/PA6/JHNPs samples.

PS/PA6/JHNPs 80/20/X phr	0 phr	1.5 phr	3 phr	5 phr	10 phr
λ_d(s)	8.9	30.0	20.8	18.2	11.0
λ_{int}(s)	[a]	[a]	176.0	136.0	156.0
$\alpha(10^{-3}$ N/m)	7.8	2.2	1.9	1.8	4.3
β''	[a]	[a]	2.6×10^{-1}	2.7×10^{-1}	3.4×10^{-1}

[a]Not evaluated.

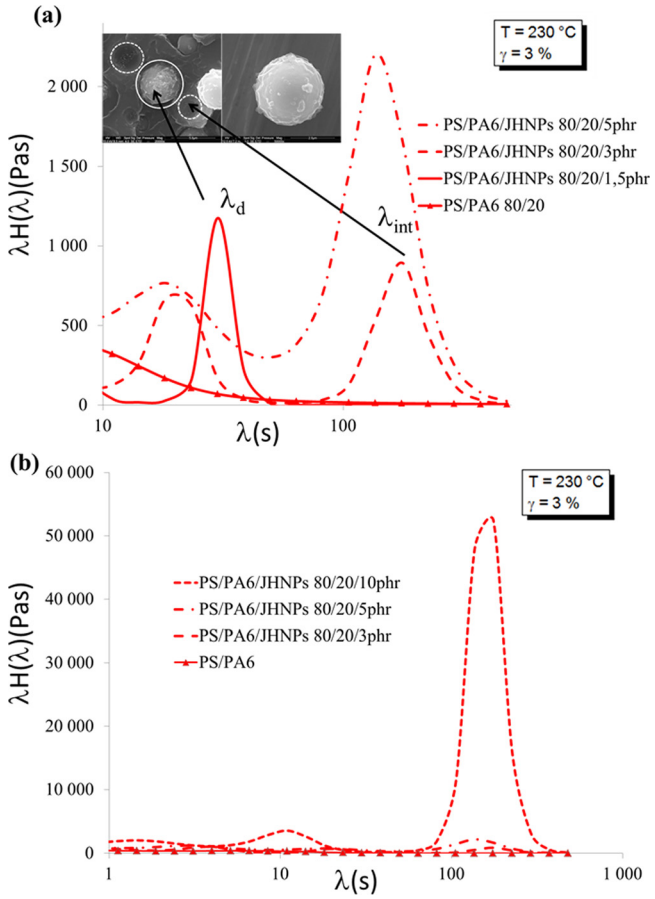

FIG. 7. Weighted relaxation spectra of PS/PA6 blends: PS/PA6 80/20, PS/PA6/JHNPs 80/20/1.5 phr, PS/PA6/JHNPs 80/20/3 phr, and PS/PA6/JHNPs 80/20/5 phr (a) and with the PS/PA6/JHNPs 80/20/10 phr bend (b) at 230 °C.

interfacial tensions from 7.4 mN/m for the neat blend to 1.95 mN/m for the nanocomposite filled with 3 phr of JHNPs. Ongoing challenge is to scale-up the quantities of the synthesized JHNPs in order to study their influence on mechanical properties and to compare it with various polymeric compatibilizers such as copolymers.

References

[1] Parpaite, T., B. Otazaghine, A. S. Caro, A. Taguet, and R. Sonnier, "Janus hybrid silica/polymer nanoparticles as effective compatibilizing agents for polystyrene/polyamide-6 melted blends," Polymer **90**, 34–44 (2016).

[2] Jacobs, U., M. Fahrlaünder, J. Winterhalter, and C. Friedrich, "Analysis of Palierne's emulsion model in the case of viscoelastic interfacial properties," J. Rheol. **43**(6), 1495–1509 (1999).

[3] Souza, A. M. C., and N. R. Demarquette, "Influence of coalescence and interfacial tension on the morphology of PP/HDPE compatibilized blends," Polymer **43**(14), 3959–3967 (2002).

[4] Jafari, S. H., A. Yavari, A. Asadinezhad, H. A. Khonakdar, and F. Böhme, "Correlation of morphology and rheological response of interfacially modified PTT/m-LLDPE blends with varying extent of modification," Polymer **46**(14), 5082–5093 (2005).

[5] Shi, D., G. H. Hu, Z. Ke, R. K. Y. Li, and J. Yin, "Relaxation behavior of polymer blends with complex morphologies: Palierne emulsion model for uncompatibilized and compatibilized PP/PA6 blends," Polymer **47**(13), 4659–4666 (2006).

[6] Chomat, D., J. Soulestin, M.-F. Lacrampe, M. Sclavons, and P. Krawczak, "In situ fibrillation of polypropylene/polyamide 6 blends: Effect of organoclay addition," J. Appl. Polym. Sci. **132**(12) 41680 (2014).

[7] Khoshnevis, H., and A. Zadhoush, "The influence of epoxy resin on the morphological and rheological properties of PET/PA66 blend," Rheol. Acta **51**(5), 467–480 (2012).

[8] Jiang, W. R., R. Y. Bao, W. Yang, Z. Y. Liu, B. H. Xie, and M. B. Yang, "Morphology, interfacial and mechanical properties of polylactide/poly(ethylene terephthalate glycol) blends compatibilized by polylactide-g-maleic anhydride," Mater. Des. **59**, 524–531 (2014).

[9] Lacroix, C., M. Aressy, and P. J. Carreau, "Linear viscoelastic behavior of molten polymer blends: A comparative study of the Palierne and Lee and Park models," Rheol. Acta **36**, 416–428 (1997).

[10] Lacroix, C., M. Bousmina, P. J. Carreau, B. D. Favis, and A. Michel, "Properties of PETG/EVA blends: 1. Viscoelastic, morphological and interfacial properties," Polymer **37**, 2939–2947 (1996).

[11] Lu, W., M. Chen, and L. Wu, "One-step synthesis of organic-inorganic hybrid asymmetric dimer particles via miniemulsion polymerization and functionalization with silver," J. Colloid Interface Sci. **328**(1), 98–102 (2008).

[12] Parpaite, T., B. Otazaghine, A. Taguet, R. Sonnier, A. S. Caro, and J. M. Lopez-Cuesta, "Incorporation of modified Stöber silica nanoparticles in polystyrene/polyamide-6 blends: Coalescence inhibition and modification of the thermal degradation via controlled dispersion at the interface," Polymer **55**(11), 2704–2715 (2014).

[13] Honerkamp, J., and J. Weese, "A nonlinear regularization method for the calculation of relaxation spectra," Rheol. Acta **32**(1), 65–73 (1993).

[14] Palierne, J. F., "Linear rheology of viscoelastic emulsions with interfacial tension," Rheol. Acta **29**(3), 204–214 (1990).

[15] Van Hemelrijck, E., P. Van Puyvelde, S. Velankar, C. W. Macosko, and P. Moldenaers, "Interfacial elasticity and coalescence suppression in compatibilized polymer blends," J. Rheol. **48**, 143–159 (2004).

[16] Wang, J., and S. Velankar, "Strain recovery of model immiscible blends without compatibilizer," Rheol. Acta **45**(3), 297–304 (2006).

[17] Favis, B. D., "Phase size/interface relationships in polymer blends: The emulsification curve," Polymer **35**, 1552–1555 (1994).

[18] Cassagnau, P., "Melt rheology of organoclay and fumed silica nanocomposites," Polymer **49**, 2183–2196 (2008).

[19] Muller, R., "Emulsion models in polymer blend rheology," in *Plastics Engineering* (Marcel Dekker Inc., New York, 1999), Vol. 52, pp. 451–474.

[20] Ville, J., P. Médéric, J. Huitric, and T. Aubry, "Structural and rheological investigation of interphase in polyethylene/polyamide/nanoclay ternary blends," Polymer **53**(8), 1733–1740 (2012).

[21] Xing, P., M. Bousmina, D. Rodrigue, and M. R. Kamal, "Critical experimental comparison between five techniques for the determination of interfacial tension in polymer blends: Model system of polystyrene/polyamide-6," Macromolecules **33**(21), 8020–8034 (2000).

[22] Brahimi, B., A. Ait-Kadi, A. Ajji, R. Jérôme, and R. Fayt, "Rheological properties of copolymer modified polyethylene/polystyrene blends," J. Rheol. **35**(6), 1069–1090 (1991).

[23] Graebling, D., "Rheological behavior of polydimethylsiloxane/polyoxyethylene blends in the melt. Emulsion model of two viscoelastic liquids," J. Rheol. **34**(2), 193–205 (1990).

[24] Gramespacher, H., "Interfacial tension between polymer melts measured by shear oscillations of their blends," J. Rheol. **36**(6), 1127–1141 (1992).